Solid Earth Discuss., 7, 1877–1908, 2015
www.solid-earth-discuss.net/7/1877/2015/
doi:10.5194/sed-7-1877-2015

Solid Earth Discussions
Open Access

Evolution of rheologically heterogeneous salt structures: a case study from the northeast of the Netherlands

A F. Raith[1], F. Strozyk[2], J. Visser[3], and J. L. Urai[1]

[1]RWTH Aachen University, Energy- and Mineral Resources Group, Structural Geology, Tectonics and Geomechanics, Aachen, Germany
[2]RWTH Aachen University, Energy and Mineral Resources Group, Geological Institute, Aachen, Germany
[3]Nedmag Industries Mining & Manufacturing B.V., Veendam, the Netherlands

Received: 27 May 2015 – Accepted: 28 May 2015 – Published: 01 July 2015

Correspondence to: A. F. Raith (a.raith@ged.rwth-aachen.de)

Published by Copernicus Publications on behalf of the European Geosciences Union.

Abstract

At the first order salt structures are controlled by the low flow strength of evaporites and by the tectonic boundary conditions. Rheological contrasts within an evaporite body have an important effect on the evolution of the internal structure of salt, but how this mechanical layering affects salt deformation at different scales is not well known. The potassium–magnesium salts (K-Mg salts) carnallite and bischofite are prime examples of layers with much lower effective viscosity than rock salt: their low viscosity presents serious drilling hazards but also allows squeeze solution mining. In contrast, anhydrite and carbonate layers (stringers) in salt are much stronger than halite. In this study, we used high-resolution 3-D seismic and well data to study the evolution of the Veendam and Slochteren salt pillows at the southern boundary of the Groningen High, northern Netherlands. Here the rock salt layers contain both the mechanically stronger Zechstein III Anhydrite–Carbonate stringer and the weaker K-Mg salts, providing an example of extreme rheological heterogeneities in salt structures. The internal structure of the two salt pillows shows areas in which the K-Mg salt-rich ZIII 1b layer is much thicker than elsewhere, in combination with a complexly ruptured and folded ZIII Anhydrite–Carbonate stringer. Thickness maps of supra-salt sediments and well data are used to infer the initial depositional architecture of the K-Mg salts and their deformation history. Results suggest that active faulting and the resulting depressions of the Zechstein surface above a Rotliegend graben caused the local accumulation of bittern brines and precipitation of the thick K-Mg salts. During the first phase of salt flow and withdrawal from the Veendam area, under differential loading by Buntsandstein sediments, the ZIII stringer was boudinaged while the lens of Mg salts remained relatively undeformed. This was followed by a convergence stage, when the K-Mg salt-rich layers were deformed with the evolving salt pillows. This deformation was strongly disharmonic and strongly influenced by folding of the underlying, ruptured ZIII stringer, leading to thickening and internal deformation of the carnallite–bischofite layers.

SED

7, 1877–1908, 2015

1 Introduction

Salt bodies are often depicted as a homogeneous mass of mechanically weak rock salt, deformed driven by buoyancy, differential loading, or gravity gliding (Jackson and Talbot, 1986; Hudec and Jackson, 2007). Our understanding of this large scale salt tectonics has grown tremendously over the last century (e.g. Jackson et al., 1996; Warren, 2006), but the internal deformation of evaporites as seen in outcrops in mines and rare surface exposures (Jackson et al., 1990) was not well known. Currently, our knowledge of this domain is making much progress, because the internal layering of salt bodies can be studied at high resolution using modern industrial 3-D seismic data (Van Gent et al., 2011; Cartwright et al., 2012; Fiduk and Rowan, 2012; Strozyk et al., 2012, 2014). In addition, the rapid development of geomechanical modelling tools (Chemia et al., 2008; Albertz et al., 2010; Albertz and Ings, 2012; Goteti et al., 2012; Li et al., 2012a, b), has allowed major contributions to this field.

Evaporites like carbonates, sulfates (anhydrite, polyhalite, tachydrite) and the K-Mg chlorides bischofite ($MgCl_2 \cdot 6H_2O$) and carnallite ($KMgCl_3 \cdot 6H_2O$) are rheologically and mechanically different from the rock salt and may have an impact on the internal deformation (Geluk, 1998; Strozyk et al., 2014). Compared to rock salt the effective viscosity of K- and Mg-salts is up to three orders of magnitude lower (Eekelen et al., 1981; Urai, 1983, 1985, 1987; Urai and Boland, 1985; Spiers et al., 1983; Langbein, 1987; Scott Duncan and Lajtai, 1993; Schenk and Urai, 2005; Urai et al., 2008), while anhydrite and carbonates have much higher viscosity than rock salt and thus form buckle folds but can also rupture in extension (Müller et al., 1981). The interaction of layers with such contrasts in rheology during deformation must lead to the development of complex fold and boudin structures, with dominant wavelength of the order of the local layer thickness. At the meso-scale, these complex internal geometries in layered evaporites are documented in mine galleries and in drill cores (Martini, 1953; Siemeister, 1969; Bornemann and Fischbeck, 1991; Burliga, 1996; Zirngast, 1996; Behlau and Mingerzahn, 2001; Bornemann et al., 2008; Schléder et al., 2008; Hammer et al., 2014). K-Mg salt-rich layers typically show complex, internal folding on the meter to mm scale, even if the entire package of layered evaporites is less deformed.

The role of high-viscosity, brittle-ductile layers (also called stringers) in salt deformation has been studied using 3-D seismic imaging (Van Gent et al., 2011; Cartwright et al., 2012; Strozyk et al., 2014), laboratory experiments, analogue models, and numerical modelling to understand the complex folds, faults, and boudinage of stringers as a result of deformation of the surrounding salt. Deformation experiments on layered salt showed the influence on rheology and the mechanics during stringer extension (Liang et al., 2007; Zulauf et al., 2010), while analogue and numerical models described the evolution of salt flow and stringer deformation (Jackson and Talbot, 1989; Koyi, 2001; Talbot and Aftabi, 2004; Zulauf and Zulauf, 2005; Chemia et al., 2008, 2009; Brun and Mauduit, 2009; Cartwright et al., 2012; Li et al., 2012a, b). In contrast, the influence of low-viscosity layers of K-Mg salts is much less understood. While in this study we focus on bischofite and carnallite, we note that other salts like tachydrite, (Poiate et al., 2006) are also very soft and have been described in evaporites offshore Brazil. The low viscosity of deeply buried K-Mg salts combined with their high solubility is a well known source of drilling problems and casing instability (Williamson et al., 1998). On the other hand, carnallite and bischofite are economically interesting and are mined in a number of locations (Vysotskiy and Kislik, 1987).

There are a few known bischofite deposits with significant thickness worldwide: in the Caspian and Kaidak basin in Kaszakhstan, the Dneiper–Donets and Pripyat in Ukraine, Gabon and Congo basin on the African platform, Sergipe basin in Brazil and the West European basin (Vysotskiy and Kislik, 1987). One of these rare occurrences of thick bischofite layers is at the southern edge of the Groningen High in the northeast of the Netherlands, where it is solution mined by the squeeze mining technique (Fokker, 1995). Bischofite is the last mineral precipitating during a full evaporation cycle (Lotze, 1957; Warren, 2006). For its precipitation out of bitterns, extremely arid conditions are required. Seawater refreshing events in salt basins normally prevent the deposition of bischofite or dissolve it, while carnallite is frequently formed (Borchert and Muir,

SED
7, 1877–1908, 2015

1964). Besides climate, tectonic processes that change the surface morphology play an important role in the depositional architecture of evaporites (Geluk et al., 2000).

In this project, we studied two salt pillows, the Veendam Pillow and Slochteren Pillow in the northeast of the Netherlands. Here, unusually thick layers of carnallite and bischofite were discovered in the Veendam Pillow in the 1970s (Coelewij et al., 1978). Today the K-Mg salts are produced by NEDMAG Industries using the squeeze mining technique (cf. Geluk et al., 2007). The bischofite layers in the Veendam Pillow are part of uppermost Zechstein III cycle, interbedded with carnallite and halite. Coelewij et al. (1978) studied this structure based on 2-D seismic data and data from wells (VDM-1 to VDM-4) on the eastern flank of the Veendam Pillow. The local Top Salt geometry and the occurrence of thick K-Mg salts were explained as result of a combination of preferential and differential salt flow. Preferential flow is caused by global differences in salt viscosity, for example due to higher temperature in the lower part of the Zechstein, causing the lower section to take up most of the strain, while the upper section folds with much less internal strain. Differential flow is caused by differences in viscosity between layers leading to local strain differences. The result of preferential flow was interpreted to cause the strong thickness variation in the ZII halite, which provides the majority of salt thickness in the salt highs. In the top part of the Zechstein section, ZIII layers of strongly different composition and viscosities are present. The high viscosity contrast between the layers was proposed to lead to strain concentrated in the softer carnallite and bischofite-rich layers. The result is the formation of “sub-pillows” of low-viscosity evaporites during halokinesis. While these interpretations represented the state of the art in the seventies, the role of sedimentary architecture causing initial thickness differences was not addressed, and no quantitative analysis or prediction of the “sub-pillows” was provided.

In summary then, study of the deformation of evaporites with extreme mechanical stratification will contribute to our understanding of salt tectonics, but also to exploration and production of potassium-magnesium salts. In addition, it helps develop the techniques to predict the internal structure of potential nuclear waste repositories in salt (Gärtner et al., 2008). In this study we address this question to gain a better understanding of the initial architecture and structural evolution, focusing on K-Mg salts and on the role of the anhydrite-carbonate stringer in the formation of internal structure.

2 Geological setting

The study area is 10 km southeast of Groningen, in the area between Veendam and Slochteren in the northeast of the Netherlands. Geologically, the area is located at the southernmost edge of the Groningen High (Fig. 1), between the northwest-southeast trending Lauwerszee Trough in the west and the Lower Saxony Basin in the southeast (Fig. 1). As part of the Lower Permian Basin it has a complex geological history with multiple tectonic phases of extension, compression, and halokinesis (Ziegler, 1978; Mohr et al., 2005; De Jager, 2007; Geluk et al., 2007). This can be summarized in four main tectonic phases (De Jager, 2007): (1) the Caledonian and Variscian orogeny during the Paleozoic caused by the assembly of the Pangea supercontinent, (2) rifting during the break up of Pangea in the Mesozoic, (3) the collision of Africa and Europe that led to the Alpine inversion during late cretaceous and early Tertiary, and (4) development of the Rhinegraben rift system in the Oligocene to recent. Key structural processes were formation and reactivation of basement faults, deformation in the Zechstein salts, and (strongly decoupled) extensional and transpressional faulting in the suprasalt sediments. Halokinesis is interpreted to have started by reactivation of basement faults, which led to differential loading and salt withdrawal (Geluk et al., 2000).

The subsalt Permian *Rotliegend* is strongly deformed by E–W and N–S to NNW–SSE striking normal and strike-slip faults that form a network of graben to half-graben structures (Fig. 1; also see De Jager, 2007; Geluk, 2007; Biehl et al., 2014).

The Zechstein section in the study area contains fully developed Z-I to Z-IV cycles. The thin and well-stratified *ZI* and lower *ZII* sequences are seismically harmonic with the Rotliegend–Zechstein contact, and are mechanically considered to be part of the

SED
7, 1877–1908, 2015

Evolution of rheologically heterogeneous salt structures

A. F. Raith et al.

subsalt. A prominent high-amplitude reflector commonly interpreted as “Base Salt” represents the transition from the ZII salt to Top ZIIC carbonates (Figs. 2 and 3). The thickness of the overlaying, seismically chaotic to transparent *ZII rock salt* varies from ca. 50 m below salt withdrawal basins up to 1.8 km in the salt pillows. In general, the ZII salts are mainly composed of halite (> 95 %; Geluk et al., 2000).

The ZIIIAC stringer represents the base of the ZIII unit and consists of the gray Salt Clay overlain by the 0.5–20 m thick Plattendolomit, and the 15–130 m thick Hauptanhydrit (Van Gent et al., 2011). As the stringer is thick and encased in rock salt, it produces a high-amplitude reflection in the seismic data (Van Gent et al., 2011; Strozyk et al., 2012, 2014).

The ZIII and ZIV units above the stringer are compositionally and mechanically layered (Coelewij et al., 1978), traditionally subdivided into several subunits (Geluk, 2007 Fig. 2). The seismically transparent lower ZIII consists of mostly halite of 100 to 300 m thickness. The ZIII-1 to -4 show a number of seismic reflectors indicating halite alternating with K-Mg salt-rich layers in the ZIII-1b, -2b and -3b. Besides halite the most common minerals here are carnallite, kieserite, and anhydrite, while in the ZIII-1b also bischofite is present (Coelewij et al., 1978). Drill cores in the study area were used to differentiate varying evaporation conditions for the ZIII-1b compared to the ZIII-2b and 3b (Coelewij et al., 1978). The ZIII-1b shows numerous alterations of bischofite, carnallite and halite as result of a regularly reversed evaporation process caused by intermittent influx of fresh seawater with a subsequent drop in salinity. The result are thin layers of simple composition which is indicative of shallow water precipitation (Coelewij et al., 1978). In the ZIII-2b and -3b on the other hand, indistinct bedding and weak development of cycles with intimate mixing of carnallite and halite crystals are the result of co-precipitation. This co-precipitation was interpreted to be caused by concentration stratification and simultaneous precipitation in two brine layers. The halite forms in the higher, less concentrated stratum, while the carnallite forms in the lower, higher-concentration/density stratum (Coelewij et al., 1978). This means that the water column during the ZIII-2b and 3b precipitation was higher than during the ZIII-1b precipitation.

SED
7, 1877–1908, 2015

Coelewij et al. (1978) used seismic acoustic impedance to evaluate the K-Mg grade of the layer. The percentage of carnallite and bischofite in a layer was interpreted to be inversely proportional to the A.I., only disturbed by the high A.I. of kieserite.

The Zechstein is overlain by Triassic (Buntsandstein and upper Röt), Cretaceous (Rijnland and Chalk) the Tertiary units (Lower/Middle and Upper North Sea Group) and the Quaternary. The Jurassic is not present in the study area (Wong, 2007).

3 Data and methods

We used two PSDM (pre-stack depth migrated) 3-D seismic volumes of different sizes and ages, provided by Nederlandse Aardolie Maatschappij (NAM). The southern seismic volume mainly covers the Veendam Pillow and has a size of 46 km^2, down to 3.25 km depth. The northern volume has a size of 135 km^2 down to 2.5 km depth (Fig. 4). Both seismic volumes overlap in the area of 30 km^2, showing vertical offsets between reflectors, due to differences in the velocity model during data processing, to be less than 30 m.

Furthermore, a total of 136 wells, including formation tops and well log data, in or close to the study area were provided by NEDMAG and the publicly available TNO online database. Well tops and well log data were mainly used for well-to-seismic tie. Especially stratigraphic boundaries of the upper Zechstein cycles (ZIII-1 to ZIV) were identified from existing well top information or have been interpreted from well logs (GR, DEN). High resolution data was available for wells TRC-1 to -9 (TRC = Tripscompagnie) and VDM-1 to -4 (VDM = Veendam).

Based on the well-to-seismic tie 15 Zechstein seismic horizons could be interpreted using Schlumberger's Petrel. Horizons were picked by a combination of manual and automated methods based on continuity and connectivity of reflectors. The interpreted horizons are Base Salt (= Top ZII-A), Top ZIII-AC ("stringer"), ZIII-1a, ZIII-1b, ZIII-2a, ZIII-2b, ZIII-3a, ZIII-3b, ZEIII-4 + ZE-IV, and Top Salt (Top ZIV). Layers ZIII-2b and ZIII-3a are not resolved in the seismic volume 2 (Figs. 2 and 3).

Major stratigraphic units in the Zechstein's overburden were interpreted to allow for a first-pass reconstruction of the study area's salt tectonic evolution: (i) Top Buntsandstein (Triassic), (ii) Top Upper Röt (Triassic), (iii) Top Upper Marl Member (Cretaceous), (iv) Top Chalk (Cretaceous), (v) Top Mid Brussels Sand Member (North Sea Supergroup), and (vi) Top Rupel Formation (North Sea Group). Additionally, one intermediate reflector in the Chalk was interpreted (Figs. 2 and 3). Thickness maps of all units were produced using Petrel's standard "stratigraphic thickness" algorithms. The thickness maps were used to identify local areas of increased sedimentation (i.e., "primary peripheral sinks"; Trusheim, 1960). During the development of salt highs these areas subside with simultaneous levelling sedimentation while the salt is migrating into the salt highs. The peripheral sinks are therefore used to identify the amount of subsidence in the sedimentary basins, the timing of their development, and their variation in spatial extent and geometry, while thinning of sediments above salt highs is used to identify reduced or non-deposition, or even uplift and erosion due to active salt doming.

4 Results

4.1 Structural overview of the study area

The *Rotliegend* is crosscut by mainly E–W and N–S to NNW–SSE striking normal and occasionally strike-slip faults (Fig. 1). The faults generally have offsets smaller than 100 m, with two larger, E–W striking normal faults bounding a 400 m deep graben below the Veendam Pillow (Fig. 1).

Morphological highs of Top Salt define two salt pillows in the study area, the Veendam Pillow (cf. Coelewij et al., 1978) and the Slochteren Pillow (Fig. 4), surrounded by salt withdrawal basins with up to 3 km post-salt sediment (Fig. 4). Post-salt sediments are generally thicker in the basins and thinner above the salt pillows (Fig. 5). The Veendam Pillow shows an elongated, SW–NE-striking geometry with 10 km length in NE–SW and 5 km width in NW–SE direction. The maximum Zechstein thickness is

SED
7, 1877–1908, 2015

2600 m, and the top of the pillow is at 1100 m depth. The Slochteren Pillow has a size of 10 km in E–W and 14 km in N–S direction, and a maximum Zechstein thickness of 1800 m at 1000 m depth below surface. In the overburden of the Slochteren pillow a large, N–S striking fault and a smaller E–W striking fault are located at its eastern and southern flank (Fig. 1).

The Top Salt surface of the two pillows is generally smooth, locally offset by faults in the post-salt sediments. These faults can be divided into two groups (Figs. 2 and 3): (1) normal faults with small offsets (< 100 m) forming grabens above the pillows, and (2) normal faults with throws that can be traced from Top Salt up to the Mid Tertiary, offsetting the postsalt sediments up to 350 m for the N–S and 200 m for the E–W-trending faults, respectively. The smaller normal faults are associated with elongated anticlines in the Top Salt surface (Fig. 6), up to 500 m wide and up to 100 m high, showing classic reactive piercement geometries (Hudec and Jackson, 2007). The crest of the Slochteren Pillow is dominated by bigger faults, without the anticline in top salt.

4.2 Stratigraphic units

4.2.1 ZIII-AC stringer

The fragmented *ZIII stringer* has an average thickness of 40 m. Below salt withdrawal basins the stringer is rather flat and parallel to Top Salt, while it shows complex patterns of rupture folding and tectonic duplication in the pillows. Fold axes have a wide range of strike, are often curved harmonic with Top Salt. N–S and EEN–WWS striking folds are more common in the Veendam Pillow, and E–W and NNW–SSE striking folds in the Slochteren Pillow. Fold amplitudes are mostly < 100 m, reaching up to 300 m in the northern flank of the Veendam Pillow. Stringer fragments that overlap a few tens of meters as well as a complex pattern of gaps are observed. In the Veendam pillow, the largest NE–SW striking gaps occur in the NW-flank of the pillow, while gaps in the center of the Slochteren pillow gaps trend towards a polygonal pattern (Fig. 7).

SED
7, 1877–1908, 2015

4.2.2 ZIII-1 to IV

The ZIII-1a, -2a, and -3a halite layers represent relatively hard units, while the K-Mg salt-rich ZIII-1b, -2b and -3b layers are relatively soft (Fig. 2). The reflectors, representing the boundaries between these units, are mostly continuous, with two exceptions: (i) reflector continuity and amplitudes decrease strongly towards the tops of salt pillows (i.e., reflectors cannot be traced in the Veendam Pillow crest, show several gaps in the Slochteren crest, and are not visible below suprasalt faults at the Slochteren Pillow), and (ii) under sedimentary basins the top ZIII-1a and Top ZIII-2a reflectors merge, and Top ZIII-1b becomes invisible. The top ZIII-1b to -3b reflectors principally follow Top Salt, and the units in between thicken towards the pillows' crests. In general, the thickness variation of < 30 m to ca. 400 m in the K-Mg salt-bearing ZIII-1b is much larger than in other units and partially correlates with the stringer geometry (Fig. 6). Thereby, the ZIII-1b is thicker above stringer fold synclines than above fold anticlines. The ZIII-1b thickness reaches its maximum above the deep stringer anticline at the north-western flank of the Veendam Pillow. In addition, the thickness of ZIII-1b is thicker directly below the small anticlines of Top Salt (see section: Discussion, Phase 3).

The ZIV generally marks Top Salt, except in parts of the Slochteren Pillow where this unit is absent.

4.2.3 Postsalt

The *Lower Triassic Buntsandstein* sediments represent the oldest Postsalt sediments above the salt with an average thickness of ca. 100 m above the Slochteren Pillow. Above the Veendam Pillow the thickness of Buntsandstein is around 400 m, with up to 550 m thickness in the surrounding basins (Fig. 5). Above the small Top Salt anticlines (see Sect. 5.2, Phase1; Fig. 6) the Buntsandstein can be 200 m thin, while adjacent to them it shows a minimum of 400 m at the western flank of the Veendam Pillow (Fig. 5). Top Bundsandstein shows a conformable contact to the Upper Triassic Upper

Röt formation, while it shows toplap contacts to the Upper Marl Member in the northern part of the study area, where the Upper Röt is missing (Fig. 5).

The *Upper Triassic Upper Röt and Solling Formation* has an average thickness of 200–300 m in the salt withdrawal basins, whereas it is significantly thinner above the Veendam Pillow (Fig. 5). It further terminates towards the north and is not present at the Slochteren Pillow (Fig. 5).

The *Cretaceous Upper Marl Member* shows a varying thickness of 50 to 140 m. In contrast to the previous units, its thickness is varying inside both the basins and above the pillows, but is not preferentially thicker in the basins (Fig. 5). The unit's contact to other units below and above is mostly concordant (Figs. 2 and 3).

The *Cretaceous Chalk* is 300 to 850 m thick and can by divided into two seismically different subunits. The lower subunit shows no significant change in thickness across the study area (Fig. 5), while the upper subunit is thicker in the salt withdrawal basins and is truncated by the Base Tertiary (Figs. 2 and 3).

The *Mid Brussels Sand Member of the Tertiary North Sea Supergroup* shows a thickness of 100 m above the pillows that increases up to 270 m in the basins (Fig. 5). The unit's top is mostly concordant to overlying strata, except at the Slochteren Pillow where toplaps in footwall position of faults are observed (Figs. 2 and 3).

The *Rupel Formation of the Tertiary North Sea Supergroup* is thick in the basins and significantly thins towards the salt pillows, where parts of the unit terminate (Fig. 5). Younger sediments are not or only partly resolved in the seismic data, and were not interpreted.

4.3 K-Mg salts in well data

Bischofite: Well data show abundant bischofite in the southern part of the study area (Fig. 4). Highest concentrations were identified in TRC wells at the eastern flank of the Veendam Pillow, where bischofite shows a cumulative thickness of up to 58 m. Significant cumulative bischofite thicknesses (i.e., < 10 m) are also present in the VDM wells, the Annerveen–Anlo (ANA -01) well at the south flank of the Veendam Pillow, and the Sappemeer (SAP) wells at the south-eastern flank of the Slochteren Pillow. Furthermore, bischofite is present with 5 m cumulative thickness in a Slochteren (SLO-01) well in the crest of the Slochteren Pillow and in the Zuiderveen (ZVN-01) well (i.e., 6 m) in a small salt high at the north-eastern boundary of the study area. Wells at the Slochteren Pillow north of SLO-01 (i.e., Froombosch (FBR), Kooipolder (KPD) and Woudbloem, WBL) show no significant bischofite occurrences. Also, no bischofite is present in the basins east of the Slochteren Pillow at Spitsbergen (SPI), Tusschenklappen (TUS) and Uiterburen (UTB), in the basin west between the two pillows at Kiel–Windeweer (KWR), and south of the Veendam Pillow at Annerveen–Wildervank (WDV).

Carnallite: Carnallite is present in all wells in the study area. Cumulative thicknesses are generally higher in the pillows than in the basins. The highest concentrations of 70–136 m cumulative thickness are found in the southern study area in TRC and VDM wells in the Veendam Pillow. South of this, thicknesses of 30 to 65 m occur. In the Slochteren Pillow, around 50 m cumulative were identified in SLO, FRB, KPD, and SAP. In the basins east of the pillow only 10 to 30 m cumulative carnallite thicknesses are present in the TUS and UTB wells.

5 Discussion

5.1 Sedimentary architecture and K-Mg salt deposition

As the K-Mg salt layers have a much lower viscosity than the halite, there is the potential for high strains in these layers. K-Mg salt distributions and thicknesses observed today may thus result from significant deformation after deposition. Therefore, the observed spatial variation in thickness can be either sedimentary or tectonic in origin, for both the carnallite and bischofite layers.

To allow for precipitation of a fully developed evaporitic cycle, including the deposition of significant amounts of bischofite, a pond-like morphological depression and

SED
7, 1877–1908, 2015

prolonged arid conditions without seawater refreshing events is required. This could have been the case above the basement graben below the study area, where subsalt faulting may have produced gentle depressions in the evolving evaporites. Recent studies showed that at least some subsalt faults in the study area were active during ZII and ZIII precipitation (Biehl et al., 2014; Strozyk et al., 2014) providing support for this. Carnallite deposited regionally as a continuous layer of varying thickness across the entire study area. Mg-enriched residual brines are interpreted to have collected inside the depression of the carnallite-rich layers above the basement graben, in the area where the Veendam Pillow later formed, with bischofite precipitation in local lenses. Smaller bischofite occurrences in other parts of the study area indicate several smaller ponds, or that later strains squeezed parts of the bischofite deposit towards some distal areas.

5.2 Salt tectonic evolution

To analyze the relative salt movements in the study area we consider the spatial and temporal changes in postsalt sediment thickness in the subsiding, evolving basins and the associated withdrawal and accumulation of salt pillows with thinning of sediments above. The resulting history of salt-sediment interaction can be summarized in three main phases (Fig. 5):

Phase 1:

During the Triassic (Buntsandstein), differential loading induced salt movement with salt withdrawal below the Veendam area and flow into the future Slochteren pillow (cf. Strozyk et al., 2014) as shown by the very different thickness distribution above both present-day pillows (Fig. 8). The significantly thinner (i.e., 100 m) Triassic sediments above the Slochteren Pillow indicate that it already formed during this early stage. Later in the Triassic, there is a reorganization of depocenters, and growth of both salt pillows in the study area. We infer that salt, withdrawn from the subsiding basins, flowed mainly from the south and the east towards the Slochteren Pillow and to a lesser degree also into the much slower evolving Veendam Pillow. During the Late Triassic, absence of

Upper Röt sediments above the Slochteren Pillow indicates continued rise of this pillow. Coevally, reactive piercement structures in Triassic sediments above the Veendam Pillow formed, forming the anticlines of Top Salt.

Phase 2:

While the Jurassic is entirely missing (cf. Wong et al., 2007), the Lower Cretaceous sediments show thicknesses of 50 to 140 m which don't show thickening above the basins. The layer has a rather continuous thickness compared to the surrounding units in the study area. Constant sediment thicknesses in the lower part of the overlying Chalk is another sign that the salt movement was very slow during a long phase.

Phase 3:

The significant thickening of upper Chalk sediments in the basins indicates renewed salt flow into the Veendam and the Slochteren pillows (Fig. 8). The rising salt lead to bending and extension in the sediments above and produced crestal collapses.

Salt tectonics continued during the Tertiary, but slowed during the deposition of the Lower North Sea Group. During deposition of the Middle and upper North Sea Group, faults above the Slochteren Pillow were active during lateral salt flow in the pillow (Figs. 2 and 3). The N–S striking and the E–W striking fault are both parallel to faults in the Base Salt at the Slochteren pillow and offset into the hanging walls. The coincidence of location, orientation and movement of faults (Fig. 5c) indicates a correlation of supra- and subsalt faulting in this area, most likely triggered from corresponding internal shear zones in the salt (also see data by Lewis et al., 2013). Post-Tertiary sediments are significantly thicker in the basins than above the pillows. This indicates ongoing salt movement into the Quaternary.

SED
7, 1877–1908, 2015

5.3 Evolution of the internal structure of the salt

In addition to the location of the bischofite layers above the subsalt graben, the second argument for a local carnallite-bischofite lens is the deformation history (as will be explained below). If the original bischofite layer would have been continuous over the study area, the first stage of deformation would have removed it from the area of the future Veendam pillow, and enriched it in the incipient Slochteren Pillow, which is not the case.

Coelewij et al. (1978) suggested that truncation of a salt body and contact with groundwater could lead to a loss of the highly soluble bischofite. However, the bischofite-rich ZIII-1b layer is not thinner towards the faults offsetting the Top Salt in Slochteren and it is more likely, that thick bischofite was not deposited here. Bischofite thickness up to 36 m in the SAP wells that are located at the south-eastern flank of the Slochteren Pillow, are interpreted as local fold hinges or boudin-necks.

As part of the salt package, the K-Mg salts can passively or actively deform in the flowing salt. The large viscosity contrast makes this possible, especially if the bischofite body is much larger than the wavelength of the fold structures so that significant stress gradients can develop to cause bischofite redistribution. Coelewij et al. (1978) suggested the thick bischofite occurrences were caused by thickening in the fold hinges. From our thickness maps however it is clear that the ZIII-1b layer's thickness does not conform to the salt pillow, it is rather located on the NW flank. This argues against redistribution over the scale of the pillow. An alternative explanation is related to the structural evolution of the anhydrite-carbonate stringer located deeper in the structure.

A closer look at the rupture pattern of the stringer shows a strikingly different pattern in the Veendam and the Slochteren pillow. In the Slochteren pillow, the rupture pattern is consistent with stretch of the layer during the rise of the pillow (Abe et al., 2013), with two major zones parallel to the crest, and smaller polygonal fractures in the crestal zone. In the Veendam pillow however, the largest ruptures are clearly off the crest of the structure. To explain these, we recall that the initial phase of salt flow was withdrawal from the Veendam area, which has led to boudinage and rupture of the stringer, before the start of growth of the Veendam pillow.

The presence of the broken stringer fragments at the start of pillow growth is interpreted to have made the internal deformation of the Veendam pillow more heterogeneous, nucleating smaller scale (few 100 m) folds to develop in the surrounding halite, which in turn formed saddle reef structures in which the bischofite was thickened. During salt flow from the location of the later Veendam Pillow towards the Slochteren Pillow the ZIII stringer is dragged with the salt and boudinaged. Later, the salt was flowing from the subsiding basins also into the Veendam Pillow, and the ZIII stringer was dragged with the salt, which locally led to compression structures like folds and thrusts. This deformation localized flows in the overlaying mobile K-Mg salts to significantly thicken above stringer synclines.

A secondary effect of the extension of Buntsandstein and the formation of reactive piercements is a reactivation of flows in topmost salts that were dragged into the bottom side of these structures. We propose that especially the highly mobile K-Mg salts filled the space formed by the faulted sediments.

While all these processes may affect the entire salt section, the low viscosity of the K-Mg-rich salts amplifies and speeds up these effects by magnitudes:

1. On large scale, K-Mg salts are passively dragged with the general salt flows, and thus preferably occur inside salt highs. Here, their thickness further increases towards the crest, which results from a radial salt flows towards the salt high's center.

2. In addition, faulting in the salt's overburden may trigger the mobile K-Mg salts to flow into the space acquired by the deformation of the overlying rocks.

3. K-Mg salts can be highly influenced by deformation of high-viscosity layers in their vicinity (e.g., anhydrite and carbonates). Folding of such layers may produce thinning and thickening of K-Mg salts on local scale.

SED
7, 1877–1908, 2015

6 Conclusions

In the northeast of the Netherlands, two Zechstein salt pillows show exceptional thickness of carnallite and bischofite in the uppermost salt section. Initial precipitation of bischofite in the area of the future Veendam Pillow occurred from Mg-rich residual brines concentrated in surface depressions above an active basement graben. The rock salt layers contain the much weaker carnallite and bischofite layers and the much stronger Zechstein III Anhydrite–Carbonate stringer, providing an example of extreme rheological heterogeneities in a salt structure.

During a first stage of salt tectonics differential loading by Triassic sediments induced salt withdrawal from the area of the future Veendam Pillow, which led to boudinage of the ZIII Anhydrite–Carbonate stringer while the K-Mg lens remained relatively undeformed. This was followed by two phases of pillow growth separated by limited salt flow during the Jurassic to mid Cretaceous. The K-Mg salt layers were deformed with the evolving salt pillows. Deformation of K-Mg salt-rich layers in the evolving salt pillows was strongly disharmonic and strongly influenced by folding of the underlying ruptured ZIII stringer. The second phase of pillow growth triggered crestal collapse above both salt anticlines and large-scale faulting above the Slochteren Pillow. The highly mobile K-Mg salts were thickened in salt anticlines below the collapse structures.

Acknowledgements. The authors thank Nedmag Industries for the financial support and further thank NEDMAG and Nederlandse Aardolie Maatschappij (NAM) for providing the data. Schlumberger is thanked for providing Petrel seismic interpretation software under academic license.

References

Abe, S., Urai, J. L., and Kettermann, M.: Fracture patterns in nonplane strain boudinage-insights from 3-D discrete element models, J. Geophys. Res.-Sol. Ea., 118, 1304–1315, doi:10.1002/jgrb.50126, 2013.

SED

7, 1877–1908, 2015

Evolution of rheologically heterogeneous salt structures

A. F. Raith et al.

Title Page
Abstract Introduction
Conclusions References
Tables Figures
◀I ▶I
◀ ▶
Back Close
Full Screen / Esc
Printer-friendly Version
Interactive Discussion

Albertz, M. and Ings, S. J.: Some consequences of mechanical stratification in basin-scale numerical models of passive-margin salt tectonics, Geol. Soc. London, Spec. Publ., 363, 303–330, doi:10.1144/SP363.14, 2012.
Albertz, M., Beaumont, C., Shimeld, J. W., Ings, S. J., and Gradmann, S.: An investigation of salt tectonic structural styles in the Scotian Basin, offshore Atlantic Canada: 1. Comparison of observations with geometrically simple numerical models, Tectonics, 29, TC4017, doi:10.1029/2009TC002539, 2010.
Behlau, J. and Mingerzahn, G.: Geological and tectonic investigations in the former Morsleben salt mine (Germany) as a basis for the safety assessment of a radioactive waste repository, Eng. Geol., 61, 83–97, doi:10.1016/S0013-7952(01)00038-2, 2001.
Biehl, B. C., Reuning, L., Strozyk, F., and Kukla, P. A.: Origin and deformation of intra-salt sulphate layers: an example from the Dutch Zechstein (Late Permian), Int. J. Earth Sci., 103, 697–712, doi:10.1007/s00531-014-0999-4, 2014.
Borchert, H. and Muir, R.: Salt Deposits: the Origin, Metamorphism and Deformation of Evaporites, D. Van Nostrand Company. Ltd, London, 1964.
Bornemann, O. and Fischbeck, R.: Zur Geologie des Salzstocks Gorleben nach den Bohrergebnissen, Deutschland Bundesamt für Strahlenschutz, Salzgitter, Germany, 1991.
Bornemann, O., Behlau, J., Fischbeck, R., Hammer, J., Jaritz, W., Keller, S., Mingerzahn, G., and Schramm, M.: Projekt Gorleben, Standortbeschreibung Gorleben. Teil 3: Ergebnisse der über- und untertägigen Erkundung des Salinars, Geologisches Jahrbuch, Bundesanstalt für Geowissenschaften und Rohstoffe (BGR), Hannover, 2008.
Brun, J. P. and Mauduit, T. P. O.: Salt rollers: structure and kinematics from analogue modelling, Mar. Petrol. Geol., 26, 249–258, doi:10.1016/j.marpetgeo.2008.02.002, 2009.
Burliga, S.: Kinematics within the Klodawa salt diapir, central Poland, Geol. Soc. London, Spec. Publ., 100, 11–21, doi:10.1144/GSL.SP.1996.100.01.02, 1996.
Cartwright, J., Jackson, M., Dooley, T., and Higgins, S.: Strain partitioning in gravity-driven shortening of a thick, multilayered evaporite sequence, Geol. Soc. London, Spec. Publ., 363, 449–470, doi:10.1144/SP363.21, 2012.
Chemia, Z., Koyi, H., and Schmeling, H.: Numerical modelling of rise and fall of a dense layer in salt diapirs, Geophys. J. Int., 172, 798–816, doi:10.1111/j.1365-246X.2007.03661.x, 2008.
Chemia, Z., Schmeling, H., and Koyi, H.: The effect of the salt viscosity on future evolution of the Gorleben salt diapir, Germany, Tectonophysics, 473, 446–456, doi:10.1016/j.tecto.2009.03.027, 2009.

Coelewij, P., Haug, G., and Van Kuijk, H.: Magnesium-salt exploration in the northeastern Netherlands, Geol. Mijnbouw., 57, 487–502, 1978.

De Jager, J.: Geological development, in: Geology of the Netherlands, edited by: Wong, T. E., Batjes, D. A. J., and De Jager, J., Royal Netherlands Academy of Arts and Sciences, 5–26, 2007.

Fiduk, J. C. and Rowan, M. G.: Analysis of folding and deformation within layered evaporites in Blocks BM-S-8 and -9, Santos Basin, Brazil, Geol. Soc. London, Spec. Publ., 363, 471–487, doi:10.1144/SP363.22, 2012.

Fokker, P. A.: The Behaviour of Salt and Salt Caverns, Dissertation, Delft University of Technology, Delft, the Netherlands, 1995.

Gärtner, G., Stockmann, N., Fricke, H., and Wallmüller, R.: Geological characterization of the Asse salt mine for mining, disposal of radioactive waste, and proof of long-term safety, in: Reviews in Engineering Geology Volume XIX: Deep Geologic Repositories, 41–52, doi:10.1130/2008.4119(05), 2008.

Geluk, M. C.: Internal tectonics of salt structures, J. Seism. Explor., 7, 237–250, 1998.

Geluk, M. C.: Permian, in: Geology of the Netherlands, edited by: Wong, T. E., Batjes, D. A. J., and De Jager, J., Royal Netherlands Academy of Arts and Sciences, 63–83, 2007.

Geluk, M. C., Röhling, H., and Brückner-Röhling, S.: Salt occurrences in the Netherlands and Germany: new insights in the formation of salt basins, in: Proceedings of the 8th World Salt Symposium, edited by: Geertman, R. M., May 2000, The Hague, Elsevier, 126–131, 2000.

Geluk, M. C., Paar, W. A., and Fokker, P. A.: Salt, in: Geology of the Netherlands, edited by: Wong, T. E., Batjes, D. A. J., and De Jager, J., Royal Netherlands Academy of Arts and Sciences, 283–294, 2007.

Goteti, R., Ings, S. J., and Beaumont, C.: Development of salt minibasins initiated by sedimentary topographic relief, Earth Planet. Sc. Lett., 339–340, 103–116, doi:10.1016/j.epsl.2012.04.045, 2012.

Hammer, J., Behlau, J., Mingerzahn, G., and Mertineit, M.: The mechanical behavior and geometry of anhydrite layers in rock salt: observations from nature, in: Natural Analogues for Safety Cases of Repositories in Rock Salt – "Salt Club" Workshop Proceedings Braunschweig, Germany, 5–7 September 2012, Hosted by Gesellschaft Für Anlagen Und Reaktorsicherheit (GRS) mbH, Braunschweig and Project Management Agency, 2014.

Hudec, M. R. and Jackson, M. P. A.: Terra infirma: understanding salt tectonics, Earth-Sci. Rev., 82, 1–28, doi:10.1016/j.earscirev.2007.01.001, 2007.

Jackson, M. and Talbot, C.: Anatomy of mushroom-shaped diapirs, J. Struct. Geol., 11, 211–230, doi:10.1016/0191-8141(89)90044-8, 1989.
Jackson, M., Roberts, D., and Snelson, S.: Salt Tectonics: a Global Perspective: Based on the Hedberg International Research Conference, Bath, UK, September 1993, Amer. Assn. of Petroleum Geologists, Tulsa, Oklahoma, USA, 1996.
Jackson, M. P. A. and Talbot, C. J.: External shapes, strain rates, and dynamics of salt structures, Geol. Soc. Am. Bull., 97, 305–323, doi:10.1130/0016-710.1130/0016-7606(1986)97<305:ESSRAD>2.0.CO;2, 1986.
Jackson, M. P. A., Cornelius, R. R., Craig, C. H., Gansser, A., Stöcklin, J., and Talbot, C. J.: 177: Salt Diapirs of the Great Kavir, Central Iran, Memoir of the Geological Society of America, doi:10.1130/MEM177, 1990.
Koyi, H. A.: Modeling the influence of sinking anhydrite blocks on salt diapirs targeted for hazardous waste disposal, Geology, 29, 387–390, doi:10.1130/0091-7613(2001)029<0387:MTIOSA>2.0.CO;2, 2001.
Langbein, R.: The Zechstein sulphates: the state of the art, in: The Zechstein Facies in Europe, Vol. 10, Springer-Verlag Berlin, Heidelberg, Germany, 143–188, 1987.
Lewis, M. M., Jackson, C. A.-L., and Gawthorpe, R. L.: Salt-influenced normal fault growth and forced folding: the Stavanger Fault System, North Sea, J. Struct. Geol., 54, 156–173, doi:10.1016/j.jsg.2013.07.015, 2013.
Li, S., Abe, S., Reuning, L., Becker, S., Urai, J. L., and Kukla, P. A.: Numerical modelling of the displacement and deformation of embedded rock bodies during salt tectonics: a case study from the South Oman Salt Basin, Geol. Soc. London, Spec. Publ., 363, 503–520, doi:10.1144/SP363.24, 2012a.
Li, S., Abe, S., Van Gent, H., Strozyk, F., Kukla, P. A., and Urai, J. L.: A method to evaluate long-term rheology of Zeichstein salt in the Tertiary, in: Mechanical Behaviour of Salt, VII, Taylor & Francis Group, London, UK, 215–220, 2012b.
Liang, W., Yang, C., Zhao, Y., Dusseault, M. B., and Liu, J.: Experimental investigation of mechanical properties of bedded salt rock, Int. J. Rock Mech. Min., 44, 400–411, doi:10.1016/j.ijrmms.2006.09.007, 2007.
Lotze, F.: Steinsalz und Kalisalze, Part I, Gebrüder Borntraeger, Berlin, 446 pp., 1957.
Martini, H. J.: Salzsättel und Deckgebirge, in: Frühjahrestagung “Salzlagerstätten” der Deutschen Geologischen Gesellschaft in Goslar, May 1953, 823–836, 1953.

SED
7, 1877–1908, 2015

Evolution of rheologically heterogeneous salt structures

A. F. Raith et al.

Mohr, M., Kukla, P. A., Urai, J. L., and Bresser, G.: Multiphase salt tectonic evolution in NW Germany: seismic interpretation and retro-deformation, Int. J. Earth Sci., 94, 917–940, doi:10.1007/s00531-005-0039-5, 2005.

Müller, W. H., Schmid, S. M., and Briegel, U.: Deformation experiments on anhydrite rocks of different grain sizes: rheology and microfabric, Tectonophysics, 78, 527–543, doi:10.1016/0040-1951(81)90027-5, 1981.

Poiate, E. J., Costa, A. M., Falcao, J. L., and Petrobrás, S. A.: Well design for drilling through thick evaporite layers in Santos Basin – Brazil, Society of Petroleum Engineers, Miami, Florida, USA, 21–23 February 2006, p. 16, doi:10.2523/99161-MS, 2006.

Schenk, O. and Urai, J. L.: The migration of fluid-filled grain boundaries in recrystallizing synthetic bischofite: first results of in-situ high-pressure, high-temperature deformation experiments in transmitted light, J. Metamorph. Geol., 23, 695–709, doi:10.1111/j.1525-1314.2005.00604.x, 2005.

Schléder, Z., Urai, J. L., Nollet, S., and Hilgers, C.: Solution-precipitation creep and fluid flow in halite: a case study of Zechstein (Z1) rocksalt from Neuhof salt mine (Germany), Int. J. Earth Sci., 97, 1045–1056, doi:10.1007/s00531-007-0275-y, 2008.

Scott Duncan, E. J. and Lajtai, E. Z.: The creep of potash salt rocks from Saskatchewan, Geotech. Geol. Eng., 11, 159–184, doi:10.1007/BF00531249, 1993.

Siemeister, G.: Primärparagenese und Metamorphose des Ronnenberglagers nach Untersuchung im Grubenfeld Salzdetfurth, Beihefte zum Geologischen Jahrbuch, Beiheft 62, Bundesanstalt für Bodenforschung, Geologische Landesämter der Bundesrepublik Deutschland, Hannover, Germany, 1969.

Spiers, C. J., Urai, J. L., Lister, G. S., Boland, J. N., and Zwart, H. J.: The influence of fluid-rock interaction on the rheology of salt rock and on ionic transport in salt, Report over the period Nov. 1981–Dec. 1983 on Radioactive waste management and disposal, HPT Laboratory, Dept. of Structural and Applied Geology, Institute of Earth Science, University of Utrecht, Utrecht, the Netherlands, 1983.

Strozyk, F., Van Gent, H., Urai, J. L., and Kukla, P. A.: 3-D seismic study of complex intra-salt deformation: an example from the Upper Permian Zechstein 3 stringer, western Dutch offshore, Geol. Soc. London, Spec. Publ., 363, 489–501, doi:10.1144/SP363.23, 2012.

Strozyk, F., Urai, J. L., Van Gent, H., De Keijzer, M., and Kukla, P. A.: The internal structure of salt?: insights from a regional 3-D seismic study of the Permian Zechstein 3 intra-salt

stringer in the Northern Netherlands, and its implications for salt tectonics, Interpretation, 2, 101–117, doi:10.1190/INT-2014-0037.1, 2014.
Talbot, C. J. and Aftabi, P.: Geology and models of salt extrusion at Qum Kuh, central Iran, J. Geol. Soc. London, 161, 321–334, doi:10.1144/0016-764903-102, 2004.
Trusheim, F.: Mechanism of salt migration in northern Germany, Am. Assoc. Petr. Geol. B, 44, 1519–1540, doi:10.1306/0BDA61CA-16BD-11D7-8645000102C1865D, 1960.
Urai, J. L., Schléder, Z., Spiers, C. J., Kukla, P. A., Lange, J.-M., and Röhling, H.-G.: Flow and Transport Properties of Salt Rocks, in: Dynamics of Complex Intracontinental Basins: The Central European Basin System, Springer Science & Business Media, 277–290, 2008.
van Eekelen, H. A., Urai, J. L., and Hulsebos, T.: Creep of bischofite, in: Proceedings, 1st Conference on the Mechanical Behaviour of Salt, Pennsylvania, 1981.
Van Gent, H., Urai, J. L., and de Keijzer, M.: The internal geometry of salt structures – a first look using 3-D seismic data from the Zechstein of the Netherlands, J. Struct. Geol., 33, 292–311, doi:10.1016/j.jsg.2010.07.005, 2011.
Vysotskiy, E. A. and Kislik, V. Z.: Epochs of bischofite deposition in geologic history, Int. Geol. Rev., 29, 134–139, doi:10.1080/00206818709466130, 1987.
Warren, J. K.: Evaporites:Sediments, Resources and Hydrocarbons, Springer Science & Business Media, Berlin Heidelberg, Germany, 2006.
Williamson, M. D., Murray, S. J., Hamilton, T. A. P., Copland, M. A.: A review of Zechstein drilling issues, in: Offshore Europe Conference in Aberdeen, Scotland, UK, 9–12 September 1997, 189–196, doi:10.2118/51182-PA, 1998.
Wong, T. E.: Jurassic, in: Geology of the Netherlands, edited by: Wong, T. E., Batjes, D. A. J., and De Jager, J., Royal Netherlands Academy of Arts and Sciences, 107–125, 2007.
Ziegler, P. A.: North-western Europe: tectonics and basin development, Geol. Mijnbouw., 57, 589–626, 1978.
Zirngast, M.: The development of the Gorleben salt dome (northwest Germany) based on quantitative analysis of peripheral sinks, Geol. Soc. London, Spec. Publ., 100, 203–226, doi:10.1144/GSL.SP.1996.100.01.13, 1996.
Zulauf, G., Zulauf, J., Bornemann, O., Brenker, F. E., Höfer, H. E., Peinl, M., and Woodland, A. B.: Experimental deformation of a single-layer anhydrite in halite matrix under bulk constriction. Part 2: Deformation mechanisms and the role of fluids, J. Struct. Geol., 32, 264–277, doi:10.1016/j.jsg.2009.12.001, 2010.

Zulauf, J. and Zulauf, G.: Coeval folding and boudinage in four dimensions, J. Struct. Geol., 27, 1061–1068, doi:10.1016/j.jsg.2005.04.003, 2005.

SED
7, 1877–1908, 2015

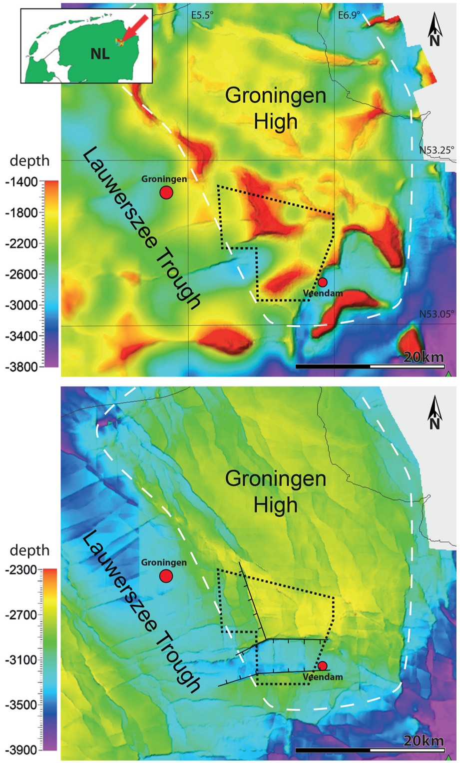

Figure 1. Top: Top salt map from the Groningen High (outline marked by with dotted line) and surrounding areas (modified after Strozyk et al., 2014). The dotted line indicates the outlines of 3-D seismic volumes covering the study area; Bottom: Base salt map from the Groningen High and surrounding areas (modified after Strozyk et al., 2014). Major normal faults (offset < 100 m) in the study area are marked.

SED
7, 1877–1908, 2015

Evolution of rheologically heterogeneous salt structures

A. F. Raith et al.

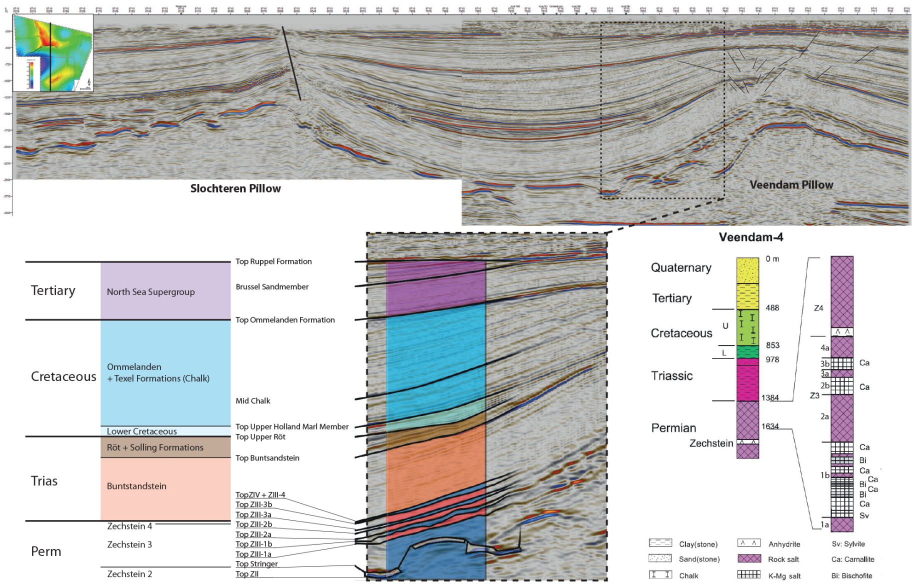

Figure 2. Top: N–S profile through the study area with the Slochteren Pillow in the north (volume 2) and the Veendam Pillow in the south (volume 1). The black lines indicate a normal fault at the south margin of the Slochteren Pillow and smaller faults above the Veendam Pillow forming a crestal collapse graben. The minibasin between the pillows shows significant thickening of most layers. The Z3 stringer is separated under the basin and folded and thrusted in the pillows. Bottom: Detailed view of interpreted stratigraphic layers and units from the Veendam Pillow and Stratigraphy of the Veendam-4 well representative for the study area (modified after Geluk et al., 2007).

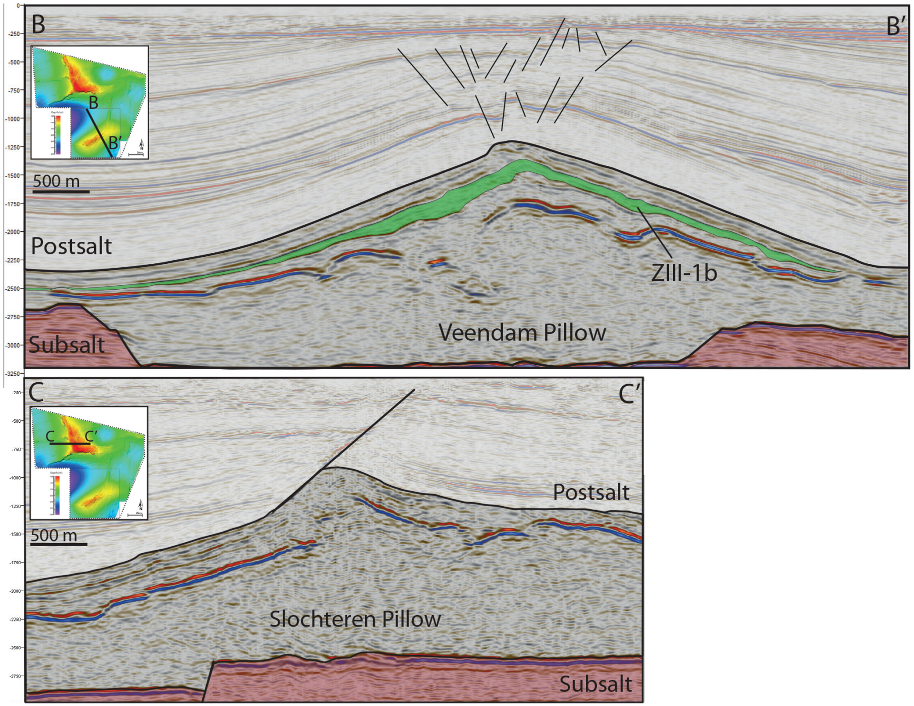

Figure 3. Top: E–W profile through the Slochteren Pillow showing the normal faults in the Sub- and Postsalt and the offset of the AC-stringer. Bottom: NNW–SSE profile through the Veendam Pillow showing thickening of the ZIII-1b (green) above the AC-stringer synclines and crestal collapse grabens above the pillow.

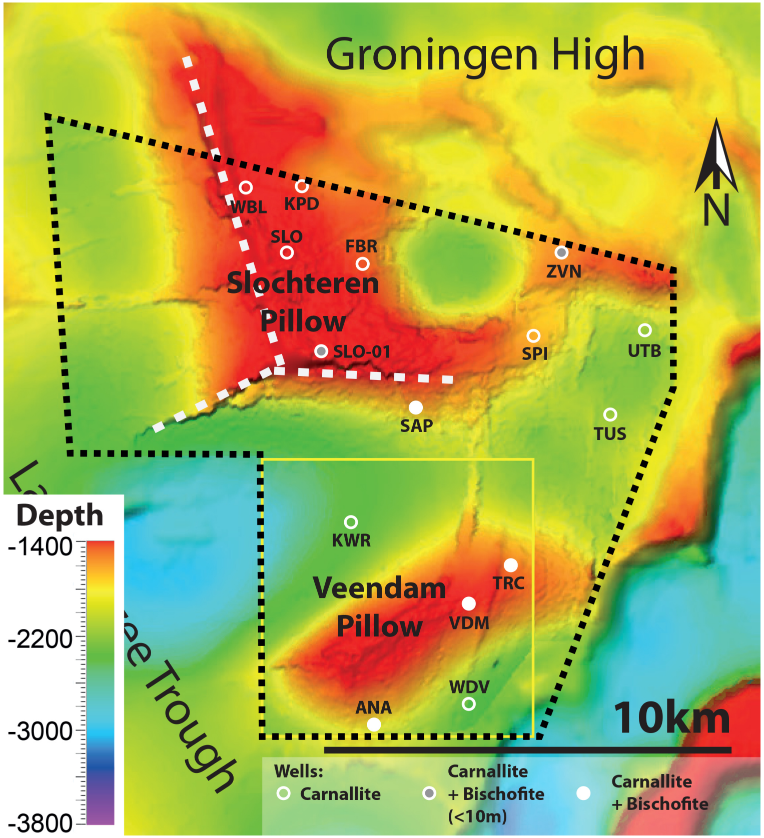

Figure 4. Top Salt surface map compiled after Strozyk et al. (2014) and this study, with well head locations. White dotted lines indicate major suprasalt faults at the Slochteren Pillow. The yellow box indicates the location of seismic volume 1.

SED
7, 1877–1908, 2015

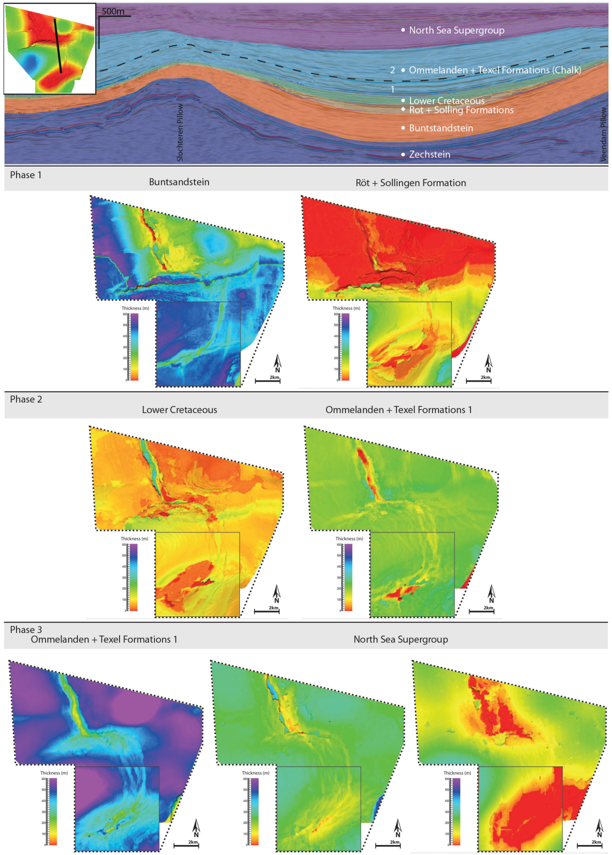

Figure 5. Supersalt thickness maps. With a profile showing the layers. Due to the influence of faults in the superasalt the thickness information in the center of the pillows is faulty. The dotted line in the chalk indicates the change from phase 2 to phase 3. The thickness maps show substantial thickening above the basins in phase 1 and 3 and constant thicknesses in phase 2.

SED
7, 1877–1908, 2015

Evolution of rheologically heterogeneous salt structures

A. F. Raith et al.

Title Page
Abstract Introduction
Conclusions References
Tables Figures
◀I ▶I
◀ ▶
Back Close
Full Screen / Esc
Printer-friendly Version
Interactive Discussion

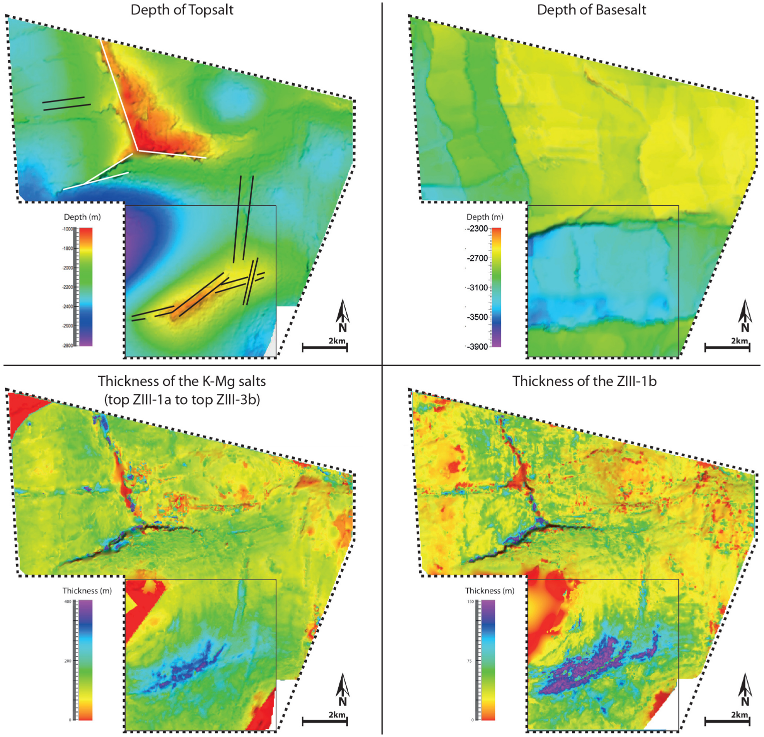

Figure 6. Detailed Top Salt map (black box indicates location of seismic volume 1) with surface inquiries (black lines) as a result of crestal collapses above salt pillows. The white lines indicate faults offsetting the Top Salt contact at the Slochteren Pillow. Thickness maps of top ZIII-1a to top ZIII-3b and top ZIII-1a to top ZIII-1b and a detailed map of the Subsalt surface (modified after Strozyk, 2014). Layers show significant thickening to the crest and under crestal collapse structures.

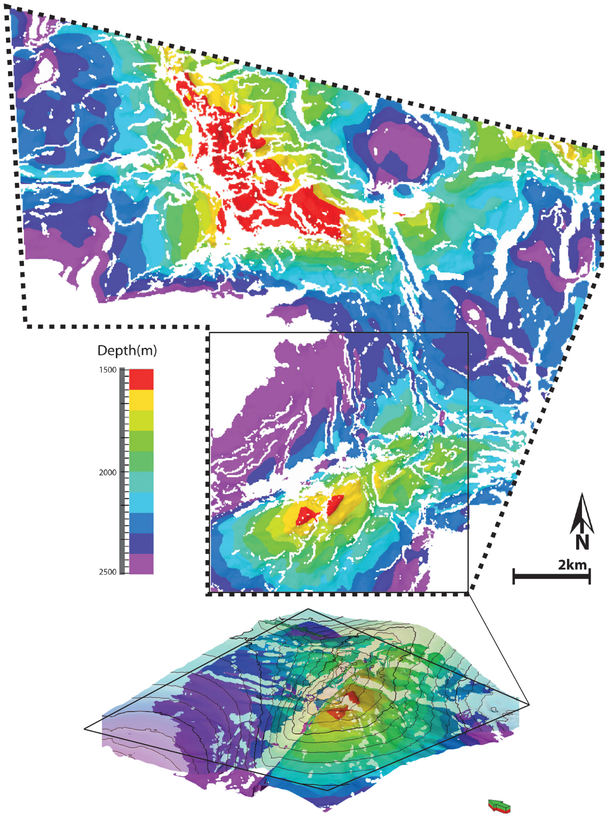

Figure 7. Map view of the ZIII stringer showing the different rupture patterns in the two pillows. The bird eyes view of the Veendam Pillow additionally shows the Topsalt surface. Here a deep stringer syncline in the NW of the Pillow is visible.

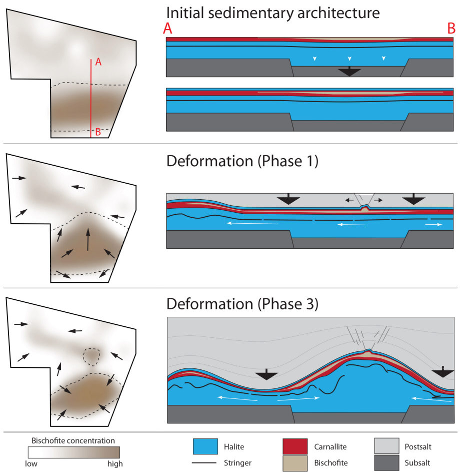

Figure 8. Conceptual reconstruction of salt deformation in the study area. The maps on the left side indicate movements in the bischofite deposit; the profile sketches **(a, b)** on the right side indicate corresponding deformation of the Zechstein (incl. ZIII stringer and K-Mg salts) and the suprasalt sediments. Black arrows indicate movements in the suprasalt sediments (e.g., extension and subsidence), white lines movements in the salt (e.g. salt withdrawal below sediment basins): **(a)** tectonic movements in the subsalt allow for localized bischofite deposition in the area of the later Veendam Pillow; **(b)** differential loading and extension in the Triassic sediments cause salt withdrawal and boudinage of the ZIII stringer in the area of the later Veendam Pillow, while salt accumulation and doming farther north triggers the formation of the Slochteren Pillow; K-Mg salts are initially deformed by extensional features in the salt's overburden; **(c)** ongoing subsidence and salt withdrawal below sedimentary basins cause the formation of the Veendam Pillow and further grow of the Slochteren Pillow. The bischofite deposits are dragged into the Veendam Pillow, where they deform due to ZIII stringer deformation and structures in the supra-salt.

SED
7, 1877–1908, 2015

Title Page
Abstract | Introduction
Conclusions | References
Tables | Figures
◂◂ | ▸▸
◂ | ▸
Back | Close
Full Screen / Esc
Printer-friendly Version
Interactive Discussion